HHS Public Access

Author manuscript

J Mol Endocrinol. Author manuscript; available in PMC 2020 July 01.

Published in final edited form as:

J Mol Endocrinol. 2019 July 01; 63(1): 11–25. doi:10.1530/JME-19-0080.

Aldose reductase regulates hyperglycemia-induced HUVEC death via SIRT1/AMPK-α1/mTOR pathway.

Pabitra B Pal[@], **Himangshu Sonowal**[@], **Kirtikar Shukla**, **Satish K Srivastava**, and **Kota V Ramana**[*]

Department of Biochemistry and Molecular Biology, University of Texas Medical Branch, Galveston, TX-77555-USA.

Abstract

Although hyperglycemia-mediated death and dysfunction of endothelial cells have been reported to be a major cause of diabetes associated vascular complications, the mechanisms through which hyperglycemia cause endothelial dysfunction is not well understood. We have recently demonstrated that aldose reductase (AR; AKR1B1) is an obligatory mediator of oxidative and inflammatory signals induced by growth factors, cytokines and hyperglycemia. However, the molecular mechanisms by which AR regulates hyperglycemia-induced endothelial dysfunction is not well known. In this study, we have investigated the mechanism(s) by which AR regulates hyperglycemia-induced endothelial dysfunction. Incubation of HUVECs with high glucose (HG) decreased the cell viability, and inhibition of AR prevented it. Further, AR inhibition prevented the HG-induced ROS generation and expression of Bcl-2, Bax, and activation of Caspase-3 in HUVECs. AR inhibition also prevented the adhesion of THP-1 monocytes on HUVECs, expression of iNOS and eNOS and adhesion molecules ICAM-1 and VCAM-1 in HG-treated HUVECs. Further, AR inhibition restored the HG-induced depletion of Sirt1 in HUVECs and increased the phosphorylation of AMPKα1 along-with a decrease in phosphorylation of mTOR in HG-treated HUVECs. Fidarestat decreased Sirt1 expression in HUVECs pre-treated with specific Sirt1 inhibitor but not with the AMPKα1 inhibitor. Similarly, knockdown of AR in HUVECs by siRNA prevented the HG-induced HUVECs cell death, THP-1 monocyte adhesion, and Sirt1 depletion. Furthermore, fidarestat regulated the phosphorylation of AMPKα1 and mTOR, and expression of Sirt1 in STZ-induced diabetic mice heart and aorta tissues. Collectively, our data suggest that AR regulates hyperglycemia-induced endothelial death and dysfunction by altering the ROS/Sirt1/AMPKα1/mTOR pathway.

[*]**Address for Correspondence:** Kota V Ramana, PhD, Dept. of Biochemistry & Molecular Biology, University of Texas Medical Branch, 6.614D Basic Science Building, 301 University Blvd. Galveston, TX 77555-0647, Tel: (409)772-2202, Fax: (409)772-9679, kvramana@utmb.edu.

Author Contributions: P.B.P performed all initial experiments and analyzed the data. H.S. helped P.B.P in animal models, performed experiments during revision and drafted the manuscript. K.S. contributed to immune blot experiments, read and provided the input on the manuscript. S.K.S. designed the study along with K.V.R and reviewed and edited the manuscript. K.V.R. designed the experimental plan, interpreted the data and prepared the final draft of the manuscript. K.V.R. is the guarantor of this work and has had full access to all the data in the study and takes responsibility for the integrity of the data and accuracy of the data analysis.

[@]Equal Contribution.

DISCLOSURE STATEMENT: The authors have nothing to disclose.

Duality of Interest: The authors declare no potential competing financial interests.

Keywords

Aldose reductase; hyperglycemia; endothelial cells; Sirt1; oxidative stress

Introduction

Hyperglycemia is a significant risk factor as well as a contributor to endothelial dysfunction and resultant cardiovascular complications frequently associated with diabetes. Generally, endothelial cells maintain the balance of cardiovascular homeostasis and act as a physical barrier between lumen and vessel wall. However, oxidative stress induced by oxidants such as hyperglycemia alters phenotypic, metabolic and signaling pathways leading to alteration of normal endothelial cell function (Pitocco et al. 2013; Tabit et al. 2010; Shukla et al.2018). Endothelial dysfunction in diabetes has been reported to be associated with the onset of secondary diabetes complications and micro- and macro-vascular diseases (Hadi and Suwaidi 2007; Sena et al. 2013; van den Oever et al. 2010).

Various strategies that alter cellular signaling pathways have been implicated in the recent past to control hyperglycemia-induced endothelial dysfunction. Specifically, conventional approaches such as insulin therapy (Franklin et al. 2008). thiazolidine-2–4-diones (TZDs) (Dandona and Aljada 2004; Freed et al. 2002; Fujishima et al. 1998). Fenofibrates which activate PPAR-α and adiponectin (Goya et al. 2004; Koh et al. 2005), and statins (Kureishi et al. 2000; Takemoto and Liao 2001) have been reported to prevent hyperglycemia-induced endothelial dysfunction. These strategies aimed at improving endothelial function by potentiating anti-oxidant defense, altering the bioavailability of Nitric Oxide (NO) in endothelial cells and improving glycemic control. However, the mechanisms by which hyperglycemia cause endothelial death and dysfunction is not well understood. Therefore, new studies are necessary to understand the mechanisms of vascular diseases and to identify new potential therapeutic targets. Recently, modulators of cellular signaling pathways, anti-inflammatory agents, and natural antioxidants have been tested for their efficacy in controlling endothelial cell dysfunction. Inhibitors of advanced glycation end-products (AGE), generation and inhibition of AGE receptor activity (Brownlee et al. 1986; Kass et al. 2001; Little et al. 2005; Stirban et al. 2006), inhibitors of protein kinase C (PKC) isoforms (Beckman et al. 2002; Vinik et al. 2005), inhibitors of vascular endothelial growth factor (VEGF) (Cunningham et al. 2005; Heier et al. 2006), anti-inflammatory drugs such as aspirin (Kern and Engerman 2001; Monobe et al. 2001), and several antioxidants such as Vitamin C, Vitamin E and plant-derived polyphenols (Engler et al. 2003; Matsumoto et al. 2003; Schini-Kerth 2014; Su 2015; Suganya et al. 2016), have been reported for their ability to improve endothelial function and protection against endothelial dysfunction in various pathologies. The NAD^+-dependent histone deacetylases such as Sirt1 have attained considerable attention as an important metabolic regulator of hyperglycemia-induced cellular dysfunction and death (Orimo et al. 2009). The AMPK-mTOR signaling axis has been reported to mediate cellular signaling pathways in response to oxidative and metabolic stresses and maintain endothelial cell function and integrity (Zou et al. 2008; Haigis and Sincalir 2010). Although these strategies have provided hope for protecting endothelial cell function, many of them have reported possible systemic and off-target side effects.

Therefore, new approaches are required to prevent hyperglycemia-induced endothelial dysfunction (Campochiaro and Group 2004; Eriksson and Nystrom 2015; Lonn et al. 2005; Miller et al. 2005).

Our recent studies have demonstrated that the polyol pathway enzyme, aldose reductase (AR), plays an important role in oxidative stress-induced pathological complications during diabetes (Srivastava et al. 2005) as well as cancer (Tammali et al. 2011). We have demonstrated that AR reduces lipid aldehydes such as 4-hydroxynonenal (4-HNE) and its glutathione conjugate GS-HNE, to their corresponding alcohols, which could act as important transducers of reactive oxygen species (ROS) -induced cellular signaling pathways. We have shown that AR inhibition prevents HG-induced VSMC proliferation by blocking the PKC and NF-κB signals (Ramana et al. 2004; Srivastava et al. 2005). Further, we have demonstrated that AR inhibitor fidarestat prevents THP-1 cells from HG-induced cell death (Shukla et al. 2017) and NLRP3 inflammasome-mediated inflammatory response (Pal et al. 2017). We have also demonstrated that AR-inhibitor fidarestat prevents chemotherapeutic drug doxorubicin-induced cardiotoxicity and endothelial dysfunction in murine models and HUVECs (Sonowal et al. 2017, Sonowal et al. 2018). However, the role of AR in hyperglycemia-induced endothelial dysfunction and cell viability is not known.

In the present study, we have demonstrated a novel role of AR in regulating hyperglycemia-induced ROS generation, HUVEC cell death, and endothelial dysfunction by controlling Sirt1 expression. Specifically, by using a combination of in vitro and in vivo models, we have demonstrated that by regulating Sirt1/AMPKα1/mTOR pathway, AR modulates hyperglycemia-induced endothelial dysfunction.

Materials and Methods

Materials

Complete Endothelial Cell Medium (ECM) was purchased from ScienCell (#1001). Streptozotocin (STZ; #S0130), D-glucose (#G7021), resveratrol (#R5010), 3-(4,5-dimethylthiazol-2-yl)-2,5-diphenyltetrazolium bromide (MTT; #M2128) were obtained from Sigma-Aldrich. AKR1B1 siRNA, control siRNA, and Hiperfect transfection reagent were obtained from Qiagen. Fidarestat was a gift from Livwell Therapeutics Inc. (CA, USA). ICAM-1 (#SC107), VCAM (#SC8304) Aldose reductase antibodies (#SC271007) and RIPA buffer were obtained from Santa Cruz Biotechnology. Antibodies against Sirt1 (#9475S), eNOS (#32027), Bcl-2 (#2872), Bax (#5023), Cytochrome c (Cyt c) (#4280), Phospho-AMPKα1 (#2537), AMPKα1 (#2795), Phospho- mTOR (#5536), mTOR (#2983), PARP (#9532), Caspase 3 (#9662), COX-IV (#4850) and GAPDH (#2118) antibodies were obtained from Cell Signaling. The iNOS (#ab129372) antibodies were obtained from Abcam. Sirt1 inhibitor III (#566322) and AMPK inhibitor (Compound C) (#171260) were obtained from Calbiochem. Calcein AM (#C3100-MP) and CM-H2DCFDA (#C6827) were obtained from Molecular Probes Invitrogen. All other chemicals and reagents were of analytical grade and were obtained from Sigma Aldrich or Thermo Fisher Scientific.

Cell culture studies

Human Umbilical Vein Endothelial Cells (HUVECs) were obtained from American Type Culture Collection (ATCC). The cells are certified free for mycoplasma and any other contaminants by ATCC and no further tests were performed in the laboratory after obtaining them. HUVECs are extensively used in the cell culture studies for performing experiments related to endothelial dysfunction and angiogenesis and show a better response to treatments as compared to other endothelial cell lines or primary cells. HUVECs were maintained in endotoxin-free endothelial cell medium (ECM) containing 5% fetal bovine serum, 1X endothelial cell growth supplement (ECGS) and penicillin-streptomycin at 37°C in a humidified atmosphere of 5% CO_2. Cells were treated with 25 mM glucose (19.5 mM glucose was added to the normal media containing 5.5 mM glucose). Control (normal media) consisted of 5.5 mM glucose. High glucose (HG; 25 mM)-treated cells were treated with or without fidarestat (10 μM) for various times periods (0–72 h). The human leukemia monocyte THP 1 cell line was obtained from American Type Culture Collection (ATCC). THP 1 monocytes were maintained in endotoxin-free RPMI 1640 medium containing 10% fetal bovine serum (FBS; Gemini Bio-Products) and penicillin-streptomycin at 37°C in a humidified atmosphere of 5% CO_2.

Cell Viability Assay

HUVECs (2×10^4 cells/mL) were cultured in ECM. Cells were seeded onto 96-well plates, and serum-starved (0.5% FBS) cells were treated with or without fidarestat (10 μM) along with high glucose in a medium containing 0.5% FBS for 24, 48 and 72 h. Cell viability was determined by 3-(4,5-dimethylthiazol-2-yl)-2,5-diphenyltetrazolium bromide (MTT) assay as described previously (Pal et al. 2017).

Live cell detection

Live cells were detected by using cell-permeable dye Calcein AM (Invitrogen, Molecular Probes). HUVECs (2×10^4 cells/mL) were seeded, and confluent cells were incubated with HG without or with fidarestat in 24-well plates for 72 h at 37°C in a CO_2 incubator. After 72 h, the cells were stained with Calcein AM (2 μM, 30 min, and 37°C), washed twice in HBSS. Fluorescence images were obtained using a fluorescence microscope. Calcein AM dye was excited at 495 nm and emission measured by using a 517 nm filter.

Annexin V/PI Staining

HUVECs were seeded onto 100 mm tissue culture dishes and allowed to adhere overnight. Cells were growth arrested in 0.5% FBS containing media without or with fidarestat (10μM). After treatment with HG (25mM) alone or in combination with fidarestat (10μM) for 48h, the cells were harvested and stained with Annexin V and Propidium Iodide (PI) for 30 min. After 30 min incubation, the cells were washed, re-suspended and data acquisition was carried out using a BD LSRII Fortessa. Data analysis was performed using Flow Jo and quadrant gates were drawn using untreated controls.

Reactive oxygen species (ROS) detection

HUVECs (2×10^4 cells/mL) were seeded, and confluent cells were incubated with HG in the presence or absence of fidarestat in 24-well plates for 24 & 48 h at 37°C in a CO_2 incubator. The cells were loaded with the fluorescent dye 5-(and-6)-chloromethyl-2′,7′-dichlorodihydrofluorescein diacetate acetyl ester (CM-H2DCFDA; 5 μM, 30mins), and washed with HBSS. Fluorescence images were obtained using a fluorescence microscope. CM-H2DCFDA dye was excited at 492–495 nm and emission measured at 517–527 nm (Pal et al. 2017).

Assay of lipid peroxidation in HUVECs

Lipid peroxidation was assayed using Image-iT Lipid peroxidation Kit form Life Technologies (Invitrogen). HUVECs were seeded onto 96-well plates and allowed to adhere overnight. Growth-arrested HUVECs were then pre-treated with fidarestat (10μM) followed by incubation with HG (25mM) in the absence or presence of fidarestat for another 24h. The cells were then loaded with 10μM lipid peroxidation sensor dye (BODIPY 581/591 C11 reagent) provided with Image-iT Lipid peroxidation Kit (Invitrogen) for 30 min. After 30min incubation, the media was removed, and the cells were washed with PBS. Fluorescence was recorded using 581/591nm (Ex/Em) (Texas Red) and 488/510nm (Ex/Em) (FITC) filters using a microplate reader (Synergy 2). Upon oxidation in live cells, the lipid peroxidation sensor dye shifts fluorescence from red (590) to green (510) and the fluorescence ratio of 590nm to 510nm provides a readout for lipid peroxidation in cells. The ratio of 590/510 is inversely proportional to lipid peroxidation.

Monocyte adhesion assay

To mimic monocyte-endothelial cell interactions in vivo, in vitro co-culture of THP-1 monocytes and HUVECs was performed to assess attachment of monocytes to HUVECs. The THP-1 monocytes were labeled with 5 μM calcein AM. Confluent HUVECs were incubated with HG in presence or absence of fidarestat in culture slides glass chamber for 48 h at 37°C in a CO_2 incubator. Subsequently, labeled THP-1 cells were added to the treated HUVEC monolayer for 12h. HG-induced expression of adhesion molecules such as ICAM, VCAM leads to the adhesion of THP-1 cells onto HUVECs. After 12h, the cells were washed gently with HBSS to remove any unattached THP-1 cells. A fluorescence microscope was used to quantify the Calcein-AM labeled THP-1 cells adhered to the HUVECs. In another set of experiments, HUVECs were incubated with high glucose without or with fidarestat in 96-well plates for 48 h at 37°C in a CO_2 incubator. Subsequently, THP-1 cells were added to the HUVECs for 12 h and washed with PBS to remove unattached cells. After washing, MTT 3-(4,5-dimethylthiazol-2-yl)-2,5-diphenyltetrazolium bromide (MTT) was added to the cells, and absorbance was recorded using a microplate reader. MTT absorbance provides an indirect measure of total live cell number in the wells.

Knockdown of aldose reductase by siRNA

HUVECs were grown in endotoxin-free endothelial cell medium containing 5% FBS, 1% endothelial cell growth supplement (ECGS) and penicillin-streptomycin at 37°C in a

humidified atmosphere of 5% CO_2. HUVECs were seeded 24 h before transfection in an appropriate culture medium containing serum and antibiotics. Cells were incubated with AR-siRNA (Predesigned siRNA against human AKR1B1, NM001628 #SI00293881, Qiagen) or control siRNA (#1022076) with HiPerFect transfection reagent to knockdown AR as per the supplier's guidelines (Qiagen). The cells were cultured for 48 h at 37°C in a humidified CO_2 incubator. The changes in the expression of AR were determined by Western blot analysis using anti–AR antibodies.

Immunofluorescence of Sirt1

To determine the localization of Sirt1 expression in cells, HUVECs were incubated with HG without or with fidarestat or resveratrol for 48 h at 37°C in a CO_2 incubator on tissue culture slides (BD Falcon). Cells were then fixed with 4% paraformaldehyde for 15 min at room temperature then washed three times in 1X PBS for 5 min each. Subsequently, the fixed cells were blocked using blocking buffer containing 5% normal goat serum for 60 min followed by incubation for overnight at 4°C with rabbit Sirt1 antibody (Cell Signaling; 1:400 dilutions in 1X PBS / 1% BSA / 0.3% Triton X-100). After washing 3x, the slides were incubated for 1 h at 37 °C with fluorochrome-conjugated secondary anti-rabbit IgG antibodies (Cell Signaling; Alexa Fluor 488 Conjugate: 1:500 dilution in 1X PBS / 1% BSA / 0.3% Triton X-100) and analyzed by fluorescence microscopy. The fluorescence intensity of the images was quantified using Image J software.

Immunoblotting

Treated HUVECs were washed with cold PBS and lysed in RIPA lysis buffer containing 1X phosphatase and protease inhibitor cocktail and centrifuged to obtain cell supernatants. Heart and aorta tissues were homogenized in RIPA buffer containing a protease inhibitor cocktail (Chem Cruz, Santa Cruz Biotechnology) with a tissue homogenizer. The tissue homogenates were centrifuged at 10,000 g for 20 min at 4°C. Total protein in the cell extracts and tissue homogenates was measured by using Bradford reagent (Bio-Rad protein assay, Bio-Rad). Equal amounts of proteins from cell lysates and tissue homogenates were subjected to SDS-PAGE followed by transfer of proteins to nitrocellulose membranes and probing with the specific antibodies. The antigen-antibody complexes were detected by enhanced Super Signal West Pico Chemiluminescent Substrate (Thermo Scientific). All blots were re-probed with GAPDH as loading control after stripping with Restore plus stripping buffer from Thermo Fisher Scientific. Densitometric analysis of western blots was performed using Image J.

Isolation of mitochondrial and cytosolic fractions

Mitochondrial as well as cytosolic fractions of HUVECs were isolated following the manufacturer's protocol using a mitochondria isolation kit from Thermo Fisher Scientific (#89874). The isolated mitochondrial and cytosolic fractions were analyzed for the expression of Bcl2, Bax, Cytc, Caspase3, PARP, COX-IV and GAPDH by immunoblotting.

Animal studies

C57BL/6 mice (male), 7- weeks old were purchased from Envigo. After one week of quarantine, mice were fed ad libitum and maintained in a specific pathogen-free environment with 12 h light/dark cycle. Mice were made diabetic by injecting a single dose of streptozotocin (STZ; 165 mg/kg, i.p.). After 5 days, blood glucose levels were measured by a glucometer (True Metrix) and only those mice which had blood glucose levels >400 mg/dL we used for further studies. Diabetic mice were randomly divided into experimental groups without or with fidarestat. In fidarestat- treated diabetic groups, fidarestat (10 mg/kg/day, i.p.) was administered to diabetic mice for 6 days, and the animals were euthanized on day 6 and tissues were collected. Aorta was obtained from another set of studies in streptozotocin (STZ; 165 mg/kg, i.p.)-induced diabetic mice treated without or with fidarestat (10 mg/kg/day, i.p.) for 21 days.

Guideline statement

All methods used in this study were performed by the guidelines and regulations approved by UTMB, Galveston. Mice were maintained in a specific pathogen-free environment at the UTMB's animal facility. The mice were randomly divided into experimental groups, and the health of the animals was frequently monitored until the end of the experiments. All animal experiments were performed in accordance with relevant guidelines and protocols approved by the Institutional Animal Care and Use Committee (IACUC), UTMB, Galveston.

Statistical analysis

Data are presented as mean± SD, and the *p* values were determined using the unpaired Student's *t*-test (GraphPad Prism software). One-way ANOVA was used for multiple comparisons. A p-value of <0.05 was considered as statistically significant.

Results:

AR inhibitor fidarestat prevents HG-induced HUVECs death and ROS formation.

We first determined the effect of AR-inhibition on HG-induced cell death in HUVECs. Results shown in Figure 1A indicate that the incubation of HUVECs with HG-resulted in a time-dependent reduction in the cell viability. The decrease in HUVECs growth was evident at 48 h and 72 h of incubation of HUVECs with HG. However, pretreatment with fidarestat significantly prevented HG-induced decrease in the HUVECs viability. Further, Calcein-AM staining of live cells after 72 h (Figure 1B) also showed a significant reduction in the cell number in HG-treated cells, but not in the HG + fidarestat treated cells. These results suggest that fidarestat prevents HG-induced endothelial cell death. The ability of fidarestat to prevent HG-induced cell death in HUVEC was further confirmed by Annexin V/PI staining. A significant increase in apoptotic cells was observed in HG-treated cells, which was prevented by fidarestat (Figure 1C and 1D). We next examined the expression of AR in HG and osmotic control mannitol treated HUVECs and diabetic mice aorta tissues. Results shown in the Supplementary Fig. 1 indicate that HG and hyperglycemia induced the expression of AR. We next analyzed the effect of fidarestat on HG-induced ROS production in HUVECs. Treatment of HUVECs with HG increased CM-H2DCFDA fluorescence, an

indicator of ROS, which was significantly prevented in the fidarestat- treated cells followed by HG (Figure 2A). No significant increase in CM-H2DCFDA fluorescence was observed in the fidarestat alone- treated cells. Further, ROS-induced lipid peroxidation was assayed in HUVECs treated with HG-alone or in combination with fidarestat. A significant increase in HG-induced lipid peroxidation was observed in HUVECs, which was prevented by fidarestat (Figure 2B).

AR inhibition prevents HG-induced apoptosis markers in HUVECs.

To further examine how AR inhibition prevents HG-induced HUVECs death, we next examined the apoptosis markers such as Bcl2, Bax and cytochrome C in mitochondrial as well as cytosolic fractions. The results shown in Figure 3A – C indicate that the incubation of HUVECs with HG increased the pro-apoptotic Bax and decreased the anti-apoptotic Bcl2 in the mitochondrial fractions. However, pretreatment of HUVECs with fidarestat reversed the HG-induced changes in the expression Bcl-2 and Bax. Resveratrol has been shown to prevent HG-induced cell death by regulating ROS and activation of SIRT1. To examine if fidarestat acts similar to resveratrol, we next pretreated HUVECs with resveratrol followed by treatment with HG and examined the expression of the apoptotic markers. Similar to fidarestat, resveratrol also prevented the HG-induced changes in the expression of apoptotic markers. To further explore the effect of fidarestat on HG-induced HUVECs cell death, we determined the mitochondria released cytochrome C, an early intermediate of apoptosis, induced by Caspase-3. Our results shown in Figure 3A (lower panel) and 3C indicate that HG increased the cytochrome C release in the cytoplasmic fractions and pretreatment of HUVECs with fidarestat or resveratrol prevented it. These results were further confirmed by determining the caspase-3 and PARP cleavage. Results shown in Figure 3A indicate that treatment of HUVECs with HG caused increased caspase-3 in the cytosol, which was prevented by fidarestat. Consistent with caspase-3 activation, HG also caused the cleavage of PARP and fidarestat prevented it. Similar to fidarestat, resveratrol also prevented the HG-induced activation of caspase-3 and PARP cleavage. These results thus suggest that fidarestat by regulating the expression of HG-induced apoptosis markers could prevent hyperglycemia-induced endothelial cell death.

Fidarestat prevents HG-induced monocyte adhesion and endothelial dysfunction

Hyperglycemia has been reported to induce endothelial dysfunction, which is one of the primary causative factors of secondary complications associated with diabetes. The role of AR in the mediation of hyperglycemia-induced monocyte adhesion to HUVECs is not known. We, therefore, analyzed the adhesion of THP-1 monocytes on HG-treated HUVEC monolayers in the absence and presence of fidarestat. The data shown in the Figure 4A indicate a significant increase in the number of Calcein-AM loaded fluorescent THP-1 cells adhered to HUVEC monolayer treated with HG, and pre-incubation of HUVECs with fidarestat prevented the THP1 cell adhesion. Similar results were observed by MTT cell viability assay, wherein, in the HG-treated group increased number of live cells were observed (indicated by an increase in MTT absorbance), and fidarestat prevented it (Figure 4B). Similar to fidarestat, resveratrol also prevented the HG-induced monocyte adhesion (Figure. 4B). We next examined the effect of HG on the expression of adhesion molecules ICAM-1, VCAM-1 and endothelial signaling mediators iNOS and eNOS in HUVECs. As

shown in Figure 4C and D, treatment of HUVECs with HG increased the expressions of ICAM-1, VCAM-1, iNOS and decreased the expression of eNOS. However, pre-incubation of HUVECs either fidarestat or resveratrol followed by HG reversed hyperglycemia-induced alteration in the expression of adhesion molecules ICAM1, VCAM1 and endothelial signaling molecules iNOS and eNOS. Thus, our results demonstrate that by preventing the expression of adhesion molecules and NOS signals, fidarestat prevents hyperglycemia-induced endothelial cell dysfunction.

AR inhibitor fidarestat regulates Sirt1 expression in HUVECs.

Our results shown in Figures 3 and 4 suggest that fidarestat is effective in preventing HG-induced endothelial cytotoxicity similar to resveratrol, a well-known activator of Sirt1, indicating that fidarestat could mediate hyperglycemia signals by regulating Sirt1 pathway. Therefore, we next examined the effect of fidarestat on the HG-induced expression of Sirt1 in HUVECs. Our results shown in Figure 5A indicate that the treatment of HUVECs with HG decreased the expression of Sirt1 and pre-treatment of HUVECs with fidarestat significantly restored the HG-induced decrease in Sirt1 expression. Further, fidarestat alone increased the expression of Sirt1 in HUVECs when compared to untreated HUVECs. Similar results were observed with resveratrol. These results were also confirmed by immunofluorescence staining (Figure 5C and 5D) using specific Sirt1 antibodies. These results suggest that fidarestat by regulating the expression of Sirt1 prevents HG-induced HUVECs death. To confirm this, we next examined how the treatment of HUVECs with a potent activator of Sirt1 (resveratrol) or inhibitor of Sirt1 (Sirt1 Inhibitor III) regulates HG-induced HUVECs growth. The results shown in Figure 5B indicate that Sirt1 activator alike fidarestat prevents HG-induced HUVECs death while Sirt1 inhibitor enhances HG-induced HUVECs death. Thus, our results demonstrate that AR inhibition could prevent hyperglycemia-induced endothelial cell death by regulating Sirt1 expression.

Fidarestat regulates HG-induced AMPKα1 and mTOR activation

AMPKα1 and mTOR share a reciprocal relationship with each other and hyperglycemia-induced activation of mTOR in endothelial cells exerts detrimental functions by inducing cellular senescence and apoptosis mediated through Sirt1. To further examine how AR regulates the HG-induced expression of Sirt1 in endothelial cells, we measured the effect of AR inhibition on HG-induced activation of AMPK and mTOR in HUVECs. The data shown in Figure 6A, indicate a time-dependent decrease in the phosphorylation of AMPKα1 in HG-treated HUVECs, which was prevented by fidarestat. Similarly, HG-induced increase in the phosphorylation of mTOR was also prevented by fidarestat. To dissect the signaling axis associated with fidarestat, Sirt1, AMPKα1, and mTOR, we used inhibitors and activators of Sirt1 and analyzed the phosphorylation of AMPKα1 and mTOR in HUVECs. Activator of Sirt1, resveratrol induced the phosphorylation of AMPKα1 and attenuated the HG-induced decrease in phosphorylation of AMPKα1, whereas an inhibitor of Sirt1 had an opposing effect (Figure. 6B). Similarly, opposing effects were observed in phosphorylation of mTOR using inhibitors and activators of Sirt1. Inhibition of Sirt1 led to an increase in phosphorylation of mTOR and augmented the HG-induced phosphorylation of mTOR, whereas activator of Sirt1 had opposing effects (Figure 6B). Further, stimulation of HUVECs with HG led to a decrease in Sirt1 expression, which was prevented by fidarestat.

However, Sirt1 expression was not affected in the presence of AMPK inhibitor. On the other hand, fidarestat decreased the Sirt1 expression in the presence of Sirt1 inhibitor-treated cells but not in the AMPKα1 inhibitor-treated cells (Figure 6C). Thus, these results indicate that by regulating AMPKα1, AR regulates the expression of Sirt1 in endothelial cells.

AR ablation prevents HUVEC death and activates Sirt1 and AMPKα1

To further confirm the role of AR in exerting protective functions against HG-induced cell death, we have ablated AR in HUVECs using specific siRNA. As shown in Figure 7A, treatment of control cells with HG decreased the HUVEC growth and knockdown of AR by siRNA protected HUVECs from HG-induced decrease in cell viability. In AR knockdown cells, resveratrol but not Sirt1 inhibitor increased the HG- decreased HUVEC growth. Further, AR knockdown cells showed resistance to HG-induced depletion of Sirt1 expression and AMPKα1 activation (Figure 7D and 7E). No differences in Sirt1 and phosphorylation of AMPKα1 were observed in control siRNA transfected cells. The expression of Sirt1 was also analyzed by immunocytochemistry in siRNA-transfected HUVECs. As shown in Figure 7B, the HG-induced decrease in Sirt1 expression in control cells but not in AR knockdown cells. Similarly, monocyte adhesion, an indicator of endothelial dysfunction, was not observed in AR knockdown HUVECs treated with HG (Figure. 7C). Further, Sirt1 inhibitor but not activator increased monocyte adhesion on HUVECs. Thus, these results suggest that AR inhibition by regulating the expression of Sirt1 prevents HG-induced endothelial cells death and dysfunction.

AR regulates the expression of Sirt1 and phosphorylation of AMPKα1 and mTOR in heart and aorta tissues of STZ-induced diabetic mice

We next examined the effect of AR-inhibition on Sirt1 expression and phosphorylation of AMPKα1 and mTOR in heart tissue lysates of STZ-induced diabetic mice. A decrease in the expression of Sirt1 and phosphorylation of AMPKα1 was observed in the heart tissue, which was restored by fidarestat (Figure 8 A, B). Similar to our in vitro results, an increase in the phosphorylation of mTOR was observed in the heart tissues of diabetic mice, which was prevented by fidarestat (Figure 8C). To analyze the long-term defects of STZ-induced hyperglycemia, we analyzed aorta tissue from 21day STZ-induced diabetic mice treated either with fidarestat or vehicle-alone. Fidarestat enhanced Sirt1 expression in the aorta of diabetic mice (Figure. 8.D). Similarly, STZ-induced decrease in phosphorylation of AMPK-α1 and increase in mTOR in the diabetic mice aorta were prevented by fidarestat (Figure 8E, F).

Discussion

The vascular endothelium is a multifunctional organ that plays an important role in paracrine, endocrine and autocrine functions and maintains vascular homeostasis under physiological conditions. Impairment of vascular endothelial function is observed in all forms of cardiovascular diseases including cardiovascular complications associated with obesity, metabolic syndrome, and type-2 diabetes. Hyperglycemia has been shown to be responsible for endothelial dysfunction leading to the onset of secondary diabetic vascular complications (Hadi and Suwaidi 2007; Sena et al. 2013; van den Oever et al. 2010).

Activation of the polyol pathway during hyperglycemia has important pathological implications. Increased glucose flux through the polyol pathway leads to alteration of cellular metabolism and generation of oxidative stress, the formation of AGE, DNA-damage and apoptosis. Several pro-inflammatory pathways are also activated by HG-through activation of NF-κB, a master regulator of pro-inflammatory and cellular signaling pathways in various cell types including endothelial cells (Ramana et al. 2004; Yerneni et al. 1999). Our past studies have demonstrated that inhibition of the polyol pathway enzyme AR, which converts glucose to sorbitol, attenuated oxidative stress-induced signaling in different pathologies including hyperglycemia (Pal et al. 2017; Ramana et al. 2004; Shukla et al. 2017; Srivastava et al. 2005; Tammali et al. 2011). Our present study indicates that inhibition of AR protects HUVECs from HG-induced endothelial cell death and dysfunction by regulating the expression of Sirt1.

Our results in this study demonstrate that AR-inhibition protects HUVECs from HG-induced endothelial dysfunction and death by signaling through ROS/Sirt1/AMPKα1/mTOR axis. Sirtuins are a family of highly conserved NAD^+-dependent histone deacetylase and have been reported to be involved in a variety of cellular processes and physiological functions such as energy metabolism, stress response, aging, tumorigenesis, etc. (Haigis and Sinclair 2010; Michan and Sinclair 2007). Sirt1 is the most evolutionary conserved mammalian sirtuin and through its NAD^+-dependent deacetylase activity can remove acetyl groups from many histone and non-histone proteins including important transcription factors such as Foxo3, p53, NF-κB, etc. (Feige and Auwerx 2008; Lee and Goldberg 2013). Sirt1 plays an essential role in hyperglycemia-induced endothelial cell dysfunction and atherosclerosis and could be a potential target to prevent the onset of diabetes-induced atherosclerosis (Yang et al. 2011). Activation of Sirt1 has been reported to protect vascular cells from hyperglycemia-induced senescence and apoptotic cell death (Hou et al. 2010; Orimo et al. 2009). Expression of Sirt1 is elevated by different anti-oxidant, anti-inflammatory and anti-diabetic compounds such as resveratrol, metformin, vitamin D, etc.

Sirtuins have also been reported to regulate the activity of AMP-activated protein kinases (AMPK) in various in vitro and in vivo models. AMPK is an important regulator of metabolic energy balance in the body. Direct and indirect activation of AMPK has been shown to exert beneficial effects in various human metabolic syndromes and cancer by targeting various upstream and downstream target genes (Kim et al. 2016; Ruderman et al. 2010). It has been shown that the overexpression of Sirt1 increases the phosphorylation of AMPK and acetyl-CoA carboxylase and siRNA mediated knockdown of Sirt1 decreases the phosphorylation of AMPK and its target genes (Lan et al. 2008). AMPK plays an important role in regulating mitochondrial homeostasis and energy balance (Herzig and Shaw 2018). Resveratrol, a potent activator of Sirt1 has been reported to induce the activation of AMPK in a Sirt1-dependent mechanism, which plays a positive role by activating mitochondrial biogenesis in the skeletal muscle cells (Price et al. 2012). Activation of AMPK by Sirt1 plays an essential role in lipid metabolism and exerts protection against high glucose-induced lipid accumulation in hepatocytes, which has important implications in diabetic atherosclerosis and age-related disorders (Hou et al. 2008). Consistent with other studies (Orimo et al. 2009), we have observed a decrease in Sirt1 expression in HG-treated endothelial cells and fidarestat upregulates the expression of the Sirt1 and prevents

endothelial cell apoptosis and endothelial dysfunction. Since inhibition of AR during hyperglycemia increases cellular NAD^+ to NADH ratio and Sirt-1 is Sirt1 is an NAD^+-dependent deacetylase, inhibition of AR exerts beneficial effects on Sirt1 activity. Studies have shown that AR also plays an important role during osmotic and oxidative stress during diabetic complications and Sirt1 regulates the expression of AR through NFAT5 in U937 monocytes (Timucin et al. 2015). Excess glucose flux through the polyol pathway has been proposed to diminish Sirt1 activation, which seems to have a possible implication in reducing vascular complications during diabetes (Vedantham et al. 2014).

Our results also suggest that AR regulates the hyperglycemia -induced expression of mammalian target of rapamycin (mTOR) in HUVECs. The mTOR signaling pathway plays an important role in cardiovascular complications associated with diabetes. A balance in mTOR activity has been shown to be essential for patients with diabetes mellitus (Chong and Maiese 2012). Activation or increase in the activity of the mTOR signaling pathway is detrimental in diabetes and is associated with the onset of cardiac hypertrophy and increased vascular cell proliferation (Chong and Maiese 2012; Shan et al. 2008). Several studies indicate that regulation of the mTOR pathway provides beneficial effects during hyperglycemia -associated cardiac and vascular dysfunctions (Ming et al. 2012). Inhibition of AMPK has been reported to induce mTOR via TCS2, which contributes to cardiac hypertrophy and insulin resistance (Kang et al. 2011). Our results demonstrate that inhibition of AR increases the phosphorylation of AMPKα1 and decreases the phosphorylation of mTOR, thus exerting protective functions under conditions of hyperglycemia, which induces mTOR and suppresses AMPKα1.

In the present study, using a combination of pharmacological and genetic approaches to silence the expression of AR under hyperglycemic conditions, we have demonstrated that AR by regulating the expression of Sirt1 via AMPKα1 and mTOR affects vascular endothelial cell functions. Although few studies have tried to correlate a signaling axis induced by osmotic stress, which regulates Sirt1 and AR (Timucin et al. 2015; Vedantham et al. 2014), we have demonstrated for the first time, a correlation between Sirt1 and AR, encompassing cellular signaling mechanism(s) which exert protective functions during hyperglycemia. Our results demonstrate a novel role of AR in regulating the expression of Sirt1 which in turn exerts a multitude of cellular protective functions to regulate endothelial function under hyperglycemia.

Supplementary Material

Refer to Web version on PubMed Central for supplementary material.

Acknowledgments:

Supported by funding from NIH/NIDDK grant DK104786.

References

Beckman JA, Goldfine AB, Gordon MB, Garrett LA & Creager MA 2002 Inhibition of protein kinase Cbeta prevents impaired endothelium-dependent vasodilation caused by hyperglycemia in humans. Circ Res 90 107–111. [PubMed: 11786526]

Brownlee M, Vlassara H, Kooney A, Ulrich P & Cerami A 1986 Aminoguanidine prevents diabetes-induced arterial wall protein cross-linking. Science 232 1629–1632. [PubMed: 3487117]

Campochiaro PA & Group CPS 2004 Reduction of diabetic macular edema by oral administration of the kinase inhibitor PKC412. Invest Ophthalmol Vis Sci 45 922–931. [PubMed: 14985312]

Chong ZZ & Maiese K 2012 Mammalian target of rapamycin signaling in diabetic cardiovascular disease. Cardiovasc Diabetol 11 45. [PubMed: 22545721]

Cunningham ET Jr., Adamis AP, Altaweel M, Aiello LP, Bressler NM, D'Amico DJ, Goldbaum M, Guyer DR, Katz B, Patel M, et al. 2005 A phase II randomized double-masked trial of pegaptanib, an anti-vascular endothelial growth factor aptamer, for diabetic macular edema. Ophthalmology 112 1747–1757. [PubMed: 16154196]

Dandona P & Aljada A 2004 Endothelial dysfunction in patients with type 2 diabetes and the effects of thiazolidinedione antidiabetic agents. J Diabetes Complications 18 91–102. [PubMed: 15120703]

Engler MM, Engler MB, Malloy MJ, Chiu EY, Schloetter MC, Paul SM, Stuehlinger M, Lin KY, Cooke JP, Morrow JD, et al. 2003 Antioxidant vitamins C and E improve endothelial function in children with hyperlipidemia: Endothelial Assessment of Risk from Lipids in Youth (EARLY) Trial. Circulation 108 1059–1063. [PubMed: 12912807]

Eriksson L & Nystrom T 2015 Antidiabetic agents and endothelial dysfunction - beyond glucose control. Basic Clin Pharmacol Toxicol 117 15–25. [PubMed: 25827165]

Feige JN & Auwerx J 2008 Transcriptional targets of sirtuins in the coordination of mammalian physiology. Curr Opin Cell Biol 20 303–309. [PubMed: 18468877]

Franklin VL, Khan F, Kennedy G, Belch JJ & Greene SA 2008 Intensive insulin therapy improves endothelial function and microvascular reactivity in young people with type 1 diabetes. Diabetologia 51 353–360. [PubMed: 18040663]

Freed MI, Ratner R, Marcovina SM, Kreider MM, Biswas N, Cohen BR, Brunzell JD & Rosiglitazone Study i 2002 Effects of rosiglitazone alone and in combination with atorvastatin on the metabolic abnormalities in type 2 diabetes mellitus. Am J Cardiol 90 947–952. [PubMed: 12398960]

Fujishima S, Ohya Y, Nakamura Y, Onaka U, Abe I & Fujishima M 1998 Troglitazone, an insulin sensitizer, increases forearm blood flow in humans. Am J Hypertens 11 1134–1137. [PubMed: 9752901]

Goya K, Sumitani S, Xu X, Kitamura T, Yamamoto H, Kurebayashi S, Saito H, Kouhara H, Kasayama S & Kawase I 2004 Peroxisome proliferator-activated receptor alpha agonists increase nitric oxide synthase expression in vascular endothelial cells. Arterioscler Thromb Vasc Biol 24 658–663. [PubMed: 14751809]

Hadi HAR & Suwaidi JA 2007 Endothelial dysfunction in diabetes mellitus. Vascular health and risk management 3 853–876. [PubMed: 18200806]

Haigis MC & Sinclair DA 2010 Mammalian sirtuins: biological insights and disease relevance. Annu Rev Pathol 5 253–295. [PubMed: 20078221]

Heier JS, Antoszyk AN, Pavan PR, Leff SR, Rosenfeld PJ, Ciulla TA, Dreyer RF, Gentile RC, Sy JP, Hantsbarger G, et al. 2006 Ranibizumab for treatment of neovascular age-related macular degeneration: a phase I/II multicenter, controlled, multidose study. Ophthalmology 113 633 e631–634. [PubMed: 16483659]

Herzig S & Shaw RJ 2018 AMPK: guardian of metabolic and mitochondrial homeostasis. Nat Rev Mol Cell Biol 19(2): 121–135 [PubMed: 28974774]

Hou J, Chong ZZ, Shang YC & Maiese K 2010 Early apoptotic vascular signaling is determined by Sirt1 through nuclear shuttling, forkhead trafficking, bad, and mitochondrial caspase activation. Curr Neurovasc Res 7 95–112. [PubMed: 20370652]

Hou X, Xu S, Maitland-Toolan KA, Sato K, Jiang B, Ido Y, Lan F, Walsh K, Wierzbicki M, Verbeuren TJ, et al. 2008 SIRT1 regulates hepatocyte lipid metabolism through activating AMP-activated protein kinase. J Biol Chem 283 20015–20026. [PubMed: 18482975]

Kang S, Chemaly ER, Hajjar RJ & Lebeche D 2011 Resistin promotes cardiac hypertrophy via the AMP-activated protein kinase/mammalian target of rapamycin (AMPK/mTOR) and c-Jun N-terminal kinase/insulin receptor substrate 1 (JNK/IRS1) pathways. J Biol Chem 286 18465–18473. [PubMed: 21478152]

Kass DA, Shapiro EP, Kawaguchi M, Capriotti AR, Scuteri A, deGroof RC & Lakatta EG 2001 Improved arterial compliance by a novel advanced glycation end-product crosslink breaker. Circulation 104 1464–1470. [PubMed: 11571237]

Kern TS & Engerman RL 2001 Pharmacological inhibition of diabetic retinopathy: aminoguanidine and aspirin. Diabetes 50 1636–1642. [PubMed: 11423486]

Kim J, Yang G, Kim Y, Kim J & Ha J 2016 AMPK activators: mechanisms of action and physiological activities. Exp Mol Med 48 e224. [PubMed: 27034026]

Koh KK, Han SH, Quon MJ, Yeal Ahn J & Shin EK 2005 Beneficial effects of fenofibrate to improve endothelial dysfunction and raise adiponectin levels in patients with primary hypertriglyceridemia. Diabetes Care 28 1419–1424. [PubMed: 15920062]

Kureishi Y, Luo Z, Shiojima I, Bialik A, Fulton D, Lefer DJ, Sessa WC & Walsh K 2000 The HMG-CoA reductase inhibitor simvastatin activates the protein kinase Akt and promotes angiogenesis in normocholesterolemic animals. Nat Med 6 1004–1010. [PubMed: 10973320]

Lan F, Cacicedo JM, Ruderman N & Ido Y 2008 SIRT1 modulation of the acetylation status, cytosolic localization, and activity of LKB1. Possible role in AMP-activated protein kinase activation. J Biol Chem 283 27628–27635. [PubMed: 18687677]

Lee D & Goldberg AL 2013 SIRT1 protein, by blocking the activities of transcription factors FoxO1 and FoxO3, inhibits muscle atrophy and promotes muscle growth. J Biol Chem 288 30515–30526. [PubMed: 24003218]

Little WC, Zile MR, Kitzman DW, Hundley WG, O'Brien TX & Degroof RC 2005 The effect of alagebrium chloride (ALT-711), a novel glucose cross-link breaker, in the treatment of elderly patients with diastolic heart failure. J Card Fail 11 191–195. [PubMed: 15812746]

Lonn E, Bosch J, Yusuf S, Sheridan P, Pogue J, Arnold JM, Ross C, Arnold A, Sleight P, Probstfield J, et al. 2005 Effects of long-term vitamin E supplementation on cardiovascular events and cancer: a randomized controlled trial. JAMA 293 1338–1347. [PubMed: 15769967]

Matsumoto T, D'Uscio LV, Eguchi D, Akiyama M, Smith LA & Katusic ZS 2003 Protective effect of chronic vitamin C treatment on endothelial function of apolipoprotein E-deficient mouse carotid artery. J Pharmacol Exp Ther 306 103–108. [PubMed: 12660308]

Michan S & Sinclair D 2007 Sirtuins in mammals: insights into their biological function. The Biochemical journal 404 1–13. [PubMed: 17447894]

Miller ER 3rd, Pastor-Barriuso R, Dalal D, Riemersma RA, Appel LJ & Guallar E 2005 Meta-analysis: high-dosage vitamin E supplementation may increase all-cause mortality. Ann Intern Med 142 37–46. [PubMed: 15537682]

Ming XF, Montani JP & Yang Z 2012 Perspectives of Targeting mTORC1-S6K1 in Cardiovascular Aging. Front Physiol 3 5. [PubMed: 22291661]

Monobe H, Yamanari H, Nakamura K & Ohe T 2001 Effects of low-dose aspirin on endothelial function in hypertensive patients. Clin Cardiol 24 705–709. [PubMed: 11714127]

Orimo M, Minamino T, Miyauchi H, Tateno K, Okada S, Moriya J & Komuro I 2009 Protective role of SIRT1 in diabetic vascular dysfunction. Arterioscler Thromb Vasc Biol 29 889–894. [PubMed: 19286634]

Pal PB, Sonowal H, Shukla K, Srivastava SK & Ramana KV 2017 Aldose Reductase Mediates NLRP3 Inflammasome-Initiated Innate Immune Response in Hyperglycemia-Induced Thp1 Monocytes and Male Mice. Endocrinology 158 3661–3675. [PubMed: 28938395]

Pitocco D, Tesauro M, Alessandro R, Ghirlanda G & Cardillo C 2013 Oxidative stress in diabetes: implications for vascular and other complications. International journal of molecular sciences 14 21525–21550. [PubMed: 24177571]

Price NL, Gomes AP, Ling AJ, Duarte FV, Martin-Montalvo A, North BJ, Agarwal B, Ye L, Ramadori G, Teodoro JS, et al. 2012 SIRT1 is required for AMPK activation and the beneficial effects of resveratrol on mitochondrial function. Cell Metab 15 675–690. [PubMed: 22560220]

Ramana KV, Friedrich B, Srivastava S, Bhatnagar A & Srivastava SK 2004 Activation of nuclear factor-kappaB by hyperglycemia in vascular smooth muscle cells is regulated by aldose reductase. Diabetes 53 2910–2920. [PubMed: 15504972]

Ruderman NB, Xu XJ, Nelson L, Cacicedo JM, Saha AK, Lan F & Ido Y 2010 AMPK and SIRT1: a long-standing partnership? Am J Physiol Endocrinol Metab 298 E751–760. [PubMed: 20103737]

Schini-Kerth V 2014 Role of polyphenols in improving endothelial dysfunction in diabetes. Free Radic Biol Med 75 Suppl 1 S11–12.

Sena CM, Pereira AM & Seica R 2013 Endothelial dysfunction - a major mediator of diabetic vascular disease. Biochim Biophys Acta 1832 2216–2231. [PubMed: 23994612]

Shan J, Nguyen TB, Totary-Jain H, Dansky H, Marx SO & Marks AR 2008 Leptin-enhanced neointimal hyperplasia is reduced by mTOR and PI3K inhibitors. Proc Natl Acad Sci U S A 105 19006–19011. [PubMed: 19020099]

Shukla K, Pal PB, Sonowal H, Srivastava SK & Ramana KV 2017 Aldose Reductase Inhibitor Protects against Hyperglycemic Stress by Activating Nrf2-Dependent Antioxidant Proteins. J Diabetes Res 6785852. [PubMed: 28740855]

Shukla K, Sonowal H, Saxena A & Ramana KV 2018 Didymin prevents hyperglycemia-induced human umbilical endothelial cells dysfunction and death. Biochemical Pharmacol. 152 1–10.

Sonowal H, Pal P, Shukla K, Saxena A, Srivastava SK & Ramana KV 2018 Aldose reductase inhibitor, fidarestat prevents doxorubicin-induced endothelial cell death and dysfunction. Biochemical Pharmacol. 150 181–190.

Sonowal H, Pal PB, Wen JJ, Awasthi S, Ramana KV & Srivastava SK 2017 Aldose reductase inhibitor increases doxorubicin-sensitivity of colon cancer cells and decreases cardiotoxicity. Sci Rep. 7(1): 3182. [PubMed: 28600556]

Srivastava SK, Ramana KV & Bhatnagar A 2005 Role of aldose reductase and oxidative damage in diabetes and the consequent potential for therapeutic options. Endocr Rev 26 380–392. [PubMed: 15814847]

Stirban A, Negrean M, Stratmann B, Gawlowski T, Horstmann T, Gotting C, Kleesiek K, Mueller-Roesel M, Koschinsky T, Uribarri J, et al. 2006 Benfotiamine prevents macro- and microvascular endothelial dysfunction and oxidative stress following a meal rich in advanced glycation end products in individuals with type 2 diabetes. Diabetes Care 29 2064–2071. [PubMed: 16936154]

Su JB 2015 Vascular endothelial dysfunction and pharmacological treatment. World J Cardiol 7 719–741. [PubMed: 26635921]

Suganya N, Bhakkiyalakshmi E, Sarada DV & Ramkumar KM 2016 Reversibility of endothelial dysfunction in diabetes: role of polyphenols. Br J Nutr 116 223–246. [PubMed: 27264638]

Tabit CE, Chung WB, Hamburg NM & Vita JA 2010 Endothelial dysfunction in diabetes mellitus: molecular mechanisms and clinical implications. Rev Endocr Metab Disord 11 61–74. [PubMed: 20186491]

Takemoto M & Liao JK 2001 Pleiotropic effects of 3-hydroxy-3-methylglutaryl coenzyme A reductase inhibitors. Arterioscler Thromb Vasc Biol 21 1712–1719. [PubMed: 11701455]

Tammali R, Srivastava SK & Ramana KV 2011 Targeting aldose reductase for the treatment of cancer. Curr Cancer Drug Targets 11 560–571. [PubMed: 21486217]

Timucin AC, Bodur C & Basaga H 2015 SIRT1 contributes to aldose reductase expression through modulating NFAT5 under osmotic stress: In vitro and in silico insights. Cell Signal 27 2160–2172. [PubMed: 26297866]

van den Oever IA, Raterman HG, Nurmohamed MT & Simsek S 2010 Endothelial dysfunction, inflammation, and apoptosis in diabetes mellitus. Mediators Inflamm 2010 792393. [PubMed: 20634940]

Vedantham S, Thiagarajan D, Ananthakrishnan R, Wang L, Rosario R, Zou YS, Goldberg I, Yan SF, Schmidt AM & Ramasamy R 2014 Aldose reductase drives hyperacetylation of Egr-1 in hyperglycemia and consequent upregulation of proinflammatory and prothrombotic signals. Diabetes 63 761–774. [PubMed: 24186862]

Vinik AI, Bril V, Kempler P, Litchy WJ, Tesfaye S, Price KL, Bastyr EJ 3rd & Group MS 2005 Treatment of symptomatic diabetic peripheral neuropathy with the protein kinase C beta-inhibitor ruboxistaurin mesylate during a 1-year, randomized, placebo-controlled, double-blind clinical trial. Clin Ther 27 1164–1180. [PubMed: 16199243]

Yang J, Wang N, Zhu Y & Feng P 2011 Roles of SIRT1 in high glucose-induced endothelial impairment: association with diabetic atherosclerosis. Arch Med Res 42 354–360. [PubMed: 21810449]

Yerneni KK, Bai W, Khan BV, Medford RM & Natarajan R 1999 Hyperglycemia-induced activation of nuclear transcription factor kappaB in vascular smooth muscle cells. Diabetes 48 855–864. [PubMed: 10102704]

Zou MH & Wu Y 2008 AMP-activated protein kinase activation as a strategy for protecting vascular endothelial function. Clin Exp Pharmacol Physiol 35 (5–6); 535–45 [PubMed: 18177481]

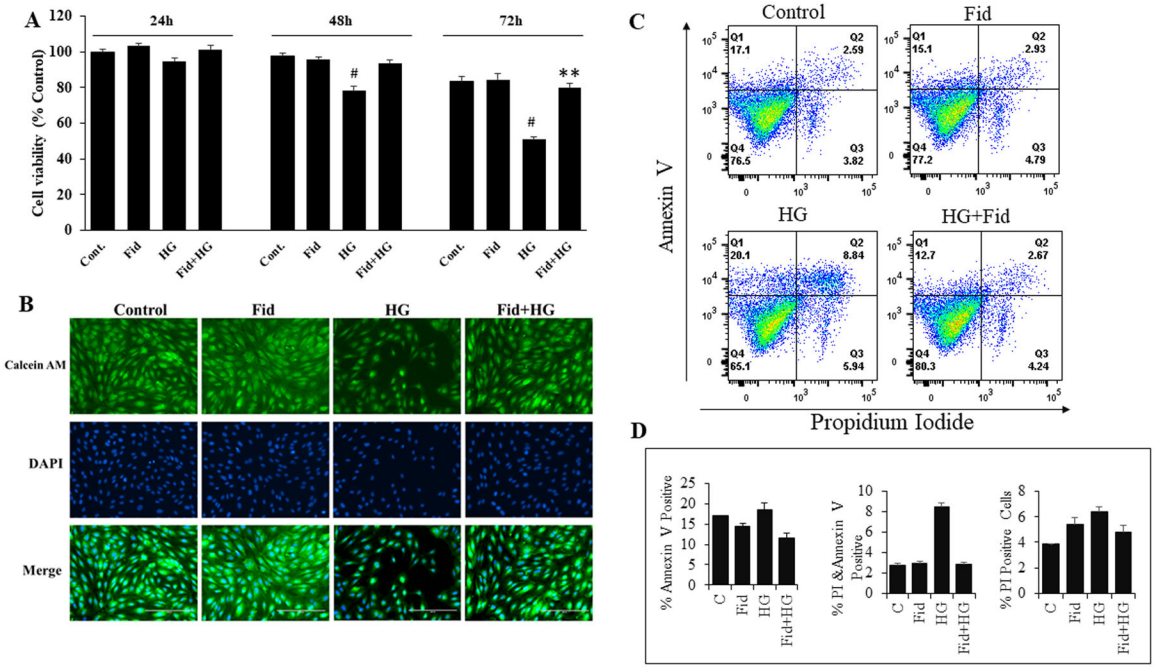

Figure. 1. Inhibition AR protects HG-induced decrease in the HUVEC viability.

(A) HUVECs were treated with HG (25 mM) without or with fidarestat (10μM) in a medium containing 0.5% FBS for 24, 48 and 72 h. Cell viability was measured by MTT assay (represented as % change over control). **(B)** HUVECs were incubated with HG without or with fidarestat in 24-well plates for 72 h at 37°C in a CO_2 incubator. After 72 h, the cells were stained with Calcein AM, washed twice in HBSS. Fluorescence images (20x) were obtained using a fluorescence microscope. **(C)** Dot plots showing Annexin V/PI stained HUVECs analyzed by flow cytometry after 48 h treatment with HG (25mM) without or with fidarestat in 0.5% FBS containing media. **(D)** Bars showing quantification of percentage Annexin V and PI positive cells in different treatment condition shown in **C**. Data acquisition was done using a BD LSRII Fortessa and analyzed by Flow Jo software. Representative data is shown. Bars represent the Mean ± SD (n =4). $^{\#}p < 0.05$ vs. Normal/ untreated control (Normal Glucose; 5.5 mM); $^{**}p < 0.01$ vs. HG (High Glucose; 19.5 mM glucose added to 5.5 mM normal glucose media).

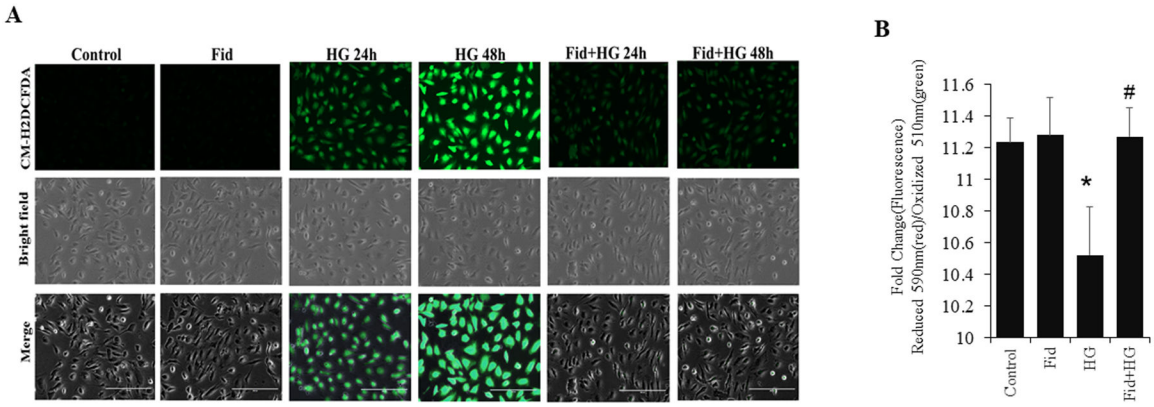

Figure. 2. AR inhibition suppresses HG-induced intracellular ROS production in HUVEC.

Growth-arrested HUVECs were incubated with high glucose (25mM) without or with fidarestat (10μM) in tissue culture plates for 24 and 48 h at 37°C in a CO_2 incubator. **(A)** Fluorescence microscopic images showing ROS in cells detected using CM-H2DCFDA dye. The cells were loaded with the fluorescent dye 5-(and-6)-chloromethyl-2′,7′-dichlorodihydrofluorescein diacetate acetyl ester (CM-H2DCFDA; 5 μM, 30min), and washed with HBSS. Fluorescence images (20x) were obtained using a fluorescence microscope. Representative images are shown. **(B)** Bars showing the ratio of fluorescence intensities in 590 (red)/510 (green) after staining with 10μM lipid peroxidation sensor dye provided with Image-iT Lipid peroxidation Kit for 30 min and recorded using a Synergy 2 microplate reader. Oxidative stress-induced oxidation of dye leads to a shift in fluorescence from red (590) to green (510) and the ratio of fluorescence intensity (590/510) provides a readout for lipid peroxidation. 590/510 ratio is inversely proportional to lipid peroxidation. Bars represent Mean±SD (n=3). Representative data is shown. *p<0.01 vs Control. #<p<0.01vs HG-treated.

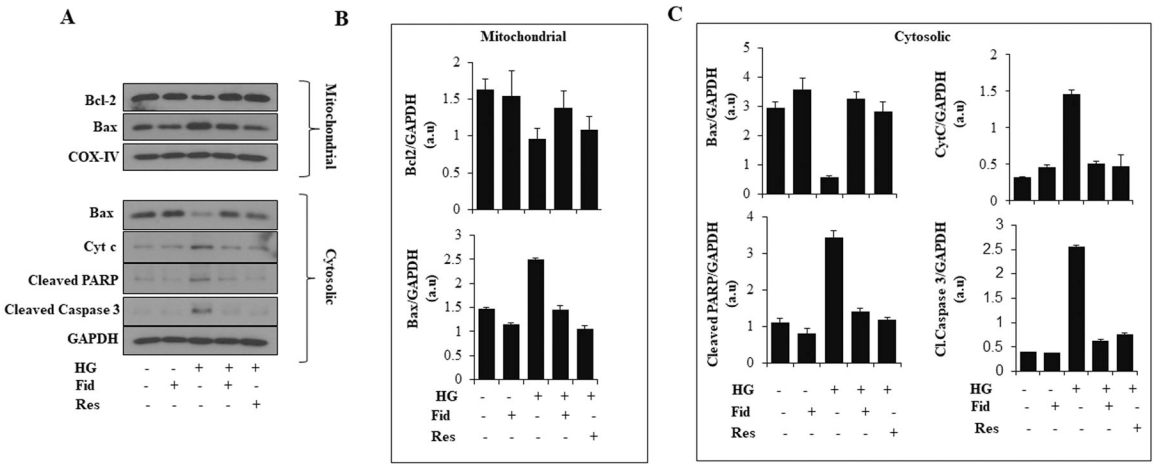

Figure. 3. AR inhibition prevents HG-induced apoptotic cell death in HUVEC:

HUVECs were incubated with HG (25 mM) without or with fidarestat (10μM) and resveratrol (20μM) for 48 h at 37°C in a CO_2 incubator. **(A)** Equal amount of proteins from the isolated mitochondrial and cytosolic fractions were used for Western blot analyses for Bcl-2, Bax, Cyt c, Cleaved PARP, Cleaved Caspase 3, COX-IV, and GAPDH. COX-IV and GAPDH were used as a loading control for mitochondrial protein and cytosolic fraction, respectively. (**B and C**) Bars representing a densitometric analysis of Western blots shown in **A**. Representative blots from the 3-independent analysis is shown.

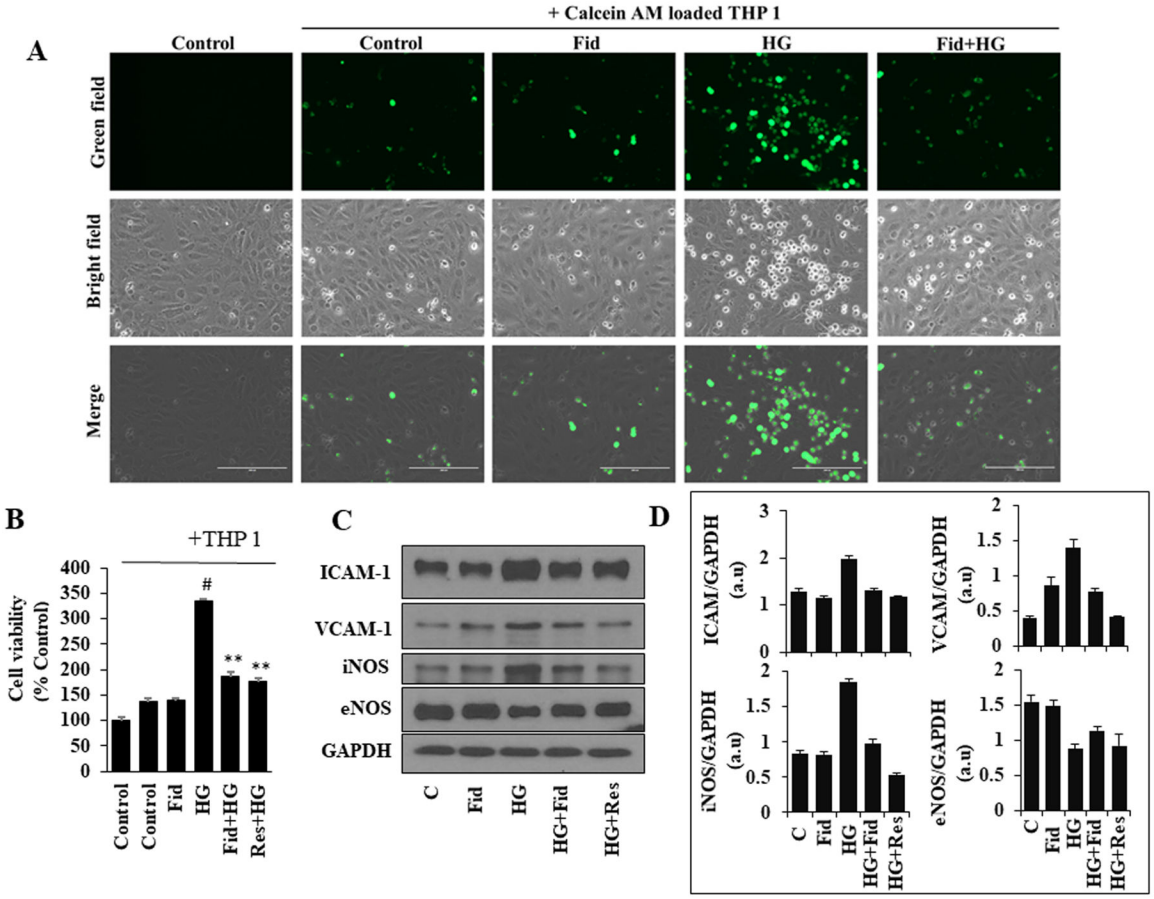

Figure. 4. Inhibition of AR prevents HG-induced monocyte adhesion and expression of adhesion molecules, eNOS, and iNOS:

(A) Growth-arrested HUVECs were incubated with HG (25mM) without or with fidarestat (10μM) in chambered tissue culture slides for 48 h at 37°C in a CO_2 incubator. Subsequently, Calcein AM-labeled THP-1 cells were added to the treated HUVECs for 12 h. The cells were then washed with HBSS. Fluorescence images (20x) were obtained using a fluorescence microscope. (**B**) HUVECs were incubated with HG without or with fidarestat (10μM) and resveratrol (Res) (20μM) in 96-well plates for 48 h at 37°C in a CO_2 incubator. Subsequently, THP-1 cells were added to the treated HUVECs for 12 h and then washed with PBS. Cell viability (% over control) was measured by MTT assay. **(C)** HUVECs were incubated with HG without or with fidarestat (10 μM) and resveratrol (20 μM) for 48 h at 37°C in a CO_2 incubator. Western blot analysis was performed by using specific ICAM-1, VCAM-1, iNOS, and eNOS antibodies. Representative blots are shown. **(D)** Bars representing a densitometric analysis of western blots shown in C. The bars represent the mean ± SD ($n = 4$). $^{\#}p < 0.05$ vs. Normal (Normal Glucose; 5.5 mM); **p < 0.01 vs. HG (High Glucose; 19.5 mM glucose added to 5.5 mM normal glucose media).

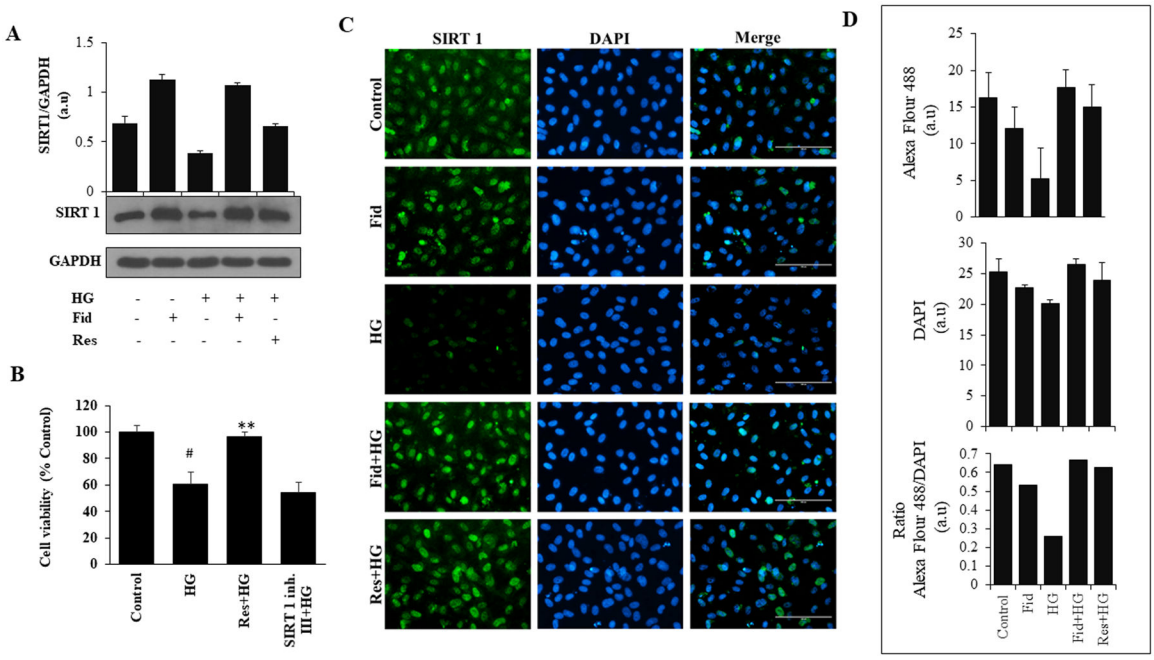

Figure. 5. Aldose reductase inhibition activates SIRT 1 in HG-induced HUVEC:

(A) Growth- arrested HUVEC cells were incubated with HG (25 mM) without or with fidarestat (10 μM) and resveratrol (20 μM) for 48 h at 37°C in a CO_2 incubator. Western blot analysis was performed by using specific Sirt1 antibodies. **(B)** HUVEC were treated with HG in the presence of Sirt1 activator (Res: 20 μM) and Sirt1 inhibitor (Sirt1 inh. III: 5μM) for 72 h. Cell viability (% over control) was measured by MTT assay. **(C)** Immunofluorescence staining was used to measure the expression for Sirt1 using antibodies against Sirt1. The images (40x) were taken in a fluorescence microscope. Scale bar=100μM. **(D)** Bars showing quantification of fluorescence intensity of Sirt1 immunofluorescence staining shown in Panel **C**. Fluorescent images were quantified using Image J software. Bars represent the mean ± SD (n =6). $^{\#}p < 0.001$ vs. Normal (Normal Glucose; 5.5 mM); $^{**}p <$ 0.001 vs. HG (High Glucose; 19.5 mM glucose added to 5.5 mM normal glucose media).

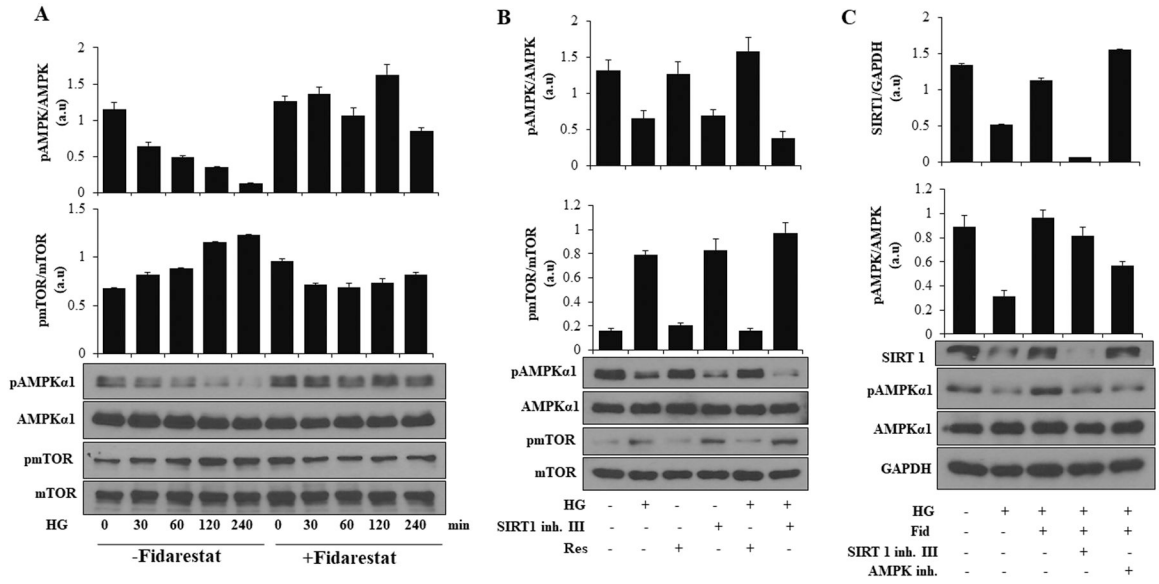

Figure. 6. AR inhibitor fidarestat regulates AMPKα1 and mTOR signaling in HUVECs:

(**A**) Growth -arrested HUVECs were pre-treated with fidarestat (10 μM) for 4 h followed by incubation with HG (25 mM) for 0, 30, 60, 120, and 240 min. Western blot analyses were performed by using specific total and phospho-AMPKα1, total AMPKα1, phospho-mTOR and total mTOR antibodies. (**B**) HUVECs were treated with HG in the absence or presence of Sirt1 activator (Res: 20 μM) and Sirt1 inhibitor (Sirt1 inh. III: 5μM) for 48 h. Western blot analyses were performed by using specific pAMPKα1, AMPKα1, phospho- mTOR, Total mTOR antibodies. (**C**) HUVECs were treated with HG without or with fidarestat followed by treatment with Sirt1 (Sirt1 inh. III: 5μM) and AMPK inhibitors (Compound C: 10 μM) for 48 h. Western blot analyses were performed by using specific Sirt1, pAMPKα1 and AMPKα1 antibodies. Representative blots from 3 independent analysis are shown.

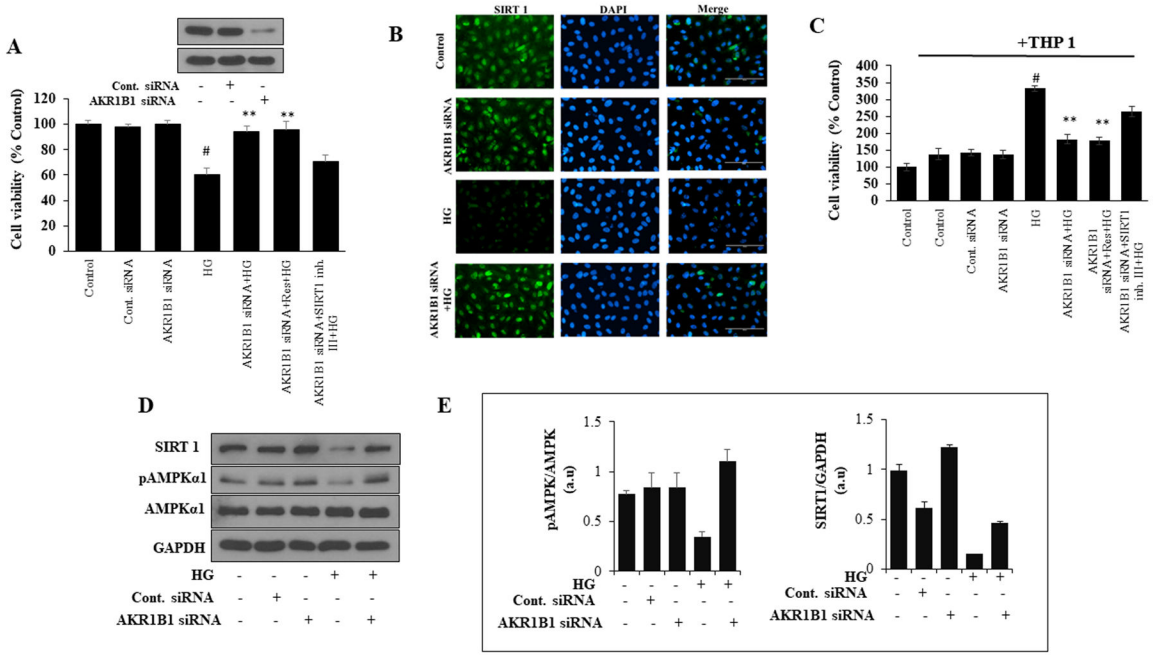

Figure. 7. Effect of AR knockdown on HUVEC cell viability, expression of Sirt1 and monocyte adhesion:

(**A**) HUVECs were transfected with AR-siRNA or control-siRNA and cultured for 48 h at 37°C. Transfected and normal cells were treated with HG in the presence or absence of Sirt1 activator (Res: 20 μM) and Sirt1 inhibitor (Sirt1 inh. III: 5μM) for 72 h. Cell viability (% over control) was measured by MTT assay. The inset shows the Western blot of AR expression in AR siRNA transfected cells. (**B**) The levels of Sirt1 protein expression was assayed by immunofluorescence staining. The images (40x) were taken in a fluorescence microscope. **(C)** AR knockdown and normal cells were treated with HG in the presence or absence of Sirt1 activator (Res: 20 μM) and Sirt1 inhibitor (Sirt1 inh.III: 5μM) for 48 h. Subsequently, THP-1 cells were added to the treated HUVECs for 12 h, washed with PBS and cell viability (% over control) was determined by MTT assay. (**D**) The AR knockdown and normal cells were treated with HG for 48h. Western blot analyses were performed by using specific Sirt1, pAMPKα1, AMPKα1 and GAPDH antibodies. (**E**). Bars showing densitometric analysis of western blots shown in D. The bars represent the mean ± SD (n=4). $^{\#}p < 0.001$ vs. Normal (Normal Glucose; 5.5 mM); $^{**}p < 0.001$ vs. HG (High Glucose; 19.5 mM glucose added to 5.5 mM normal glucose media).

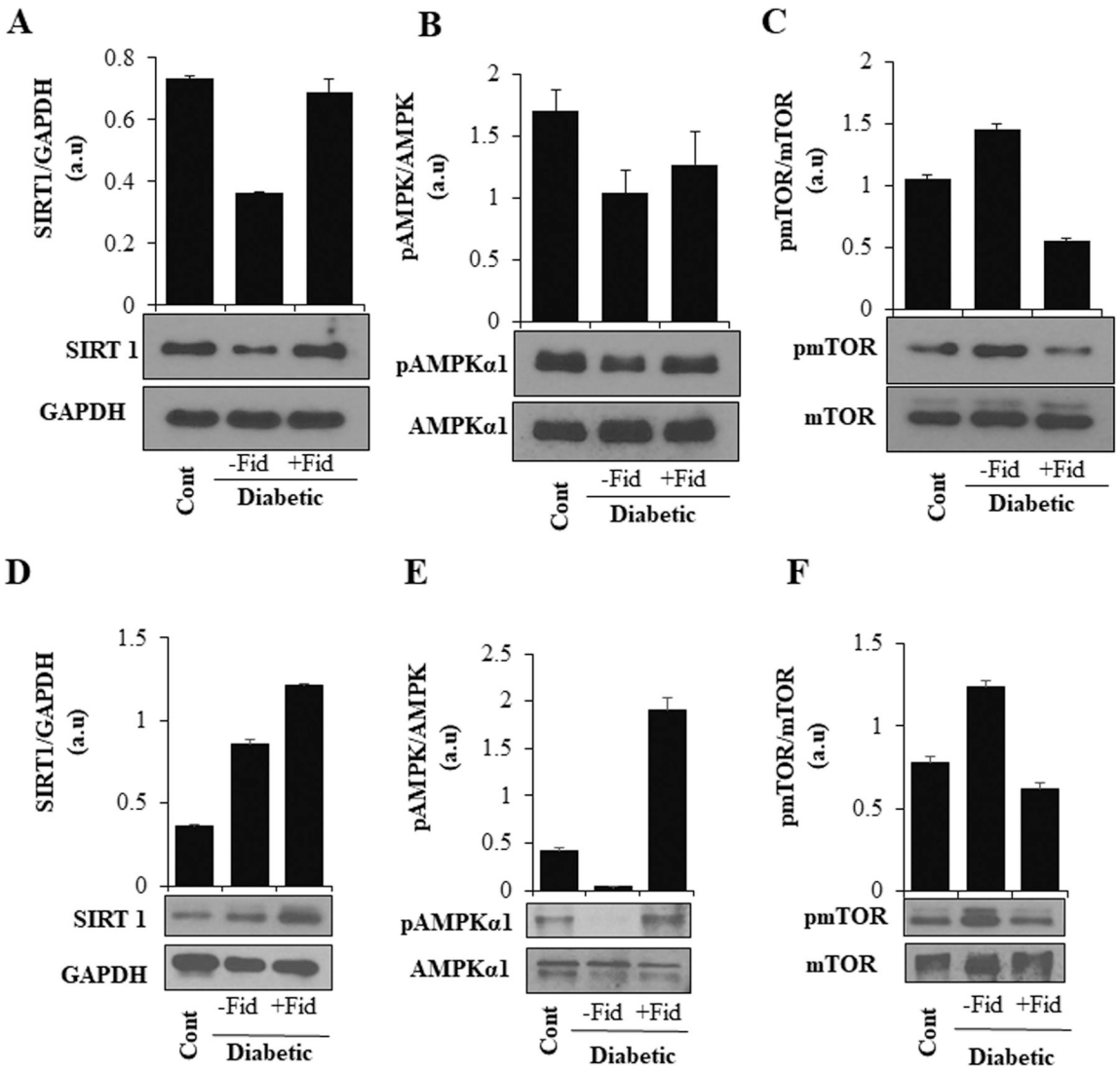

Figure. 8. AR inhibition increased the expression of Sirt1, pAMPKα1 and decreased pmTOR expression in STZ- induced diabetic mice hearts and aorta:

Male C57BL/6 mice were made diabetic as described in the methods. The diabetic mice were treated with fidarestat (10mg/kg/day i.p) for 6 days. The levels of (**A**) Sirt1, (**B**) pAMPKα1 and (**C**) pmTOR proteins were measured in heart tissues by Western blot analysis using specific antibodies. In another set of experiments, diabetic mice were treated with AR-inhibitor fidarestat for 21 days (10mg/kg/day i.p). Thoracic aorta tissue sections were dissected and lysed and analyzed by western blotting using specific antibodies for **(D)** SIRT1 **(E)** p-AMPKα1 and **(F)** p-mTOR. A representative blot from each group is shown.